Nitrate salt-halloysite nanotube (HNT) composite phase change materials for thermal energy storage: The feasibility of material fabrication by using HNT as skeleton substance and its thermal properties

Chuan Li [a], Li Han [a], Guoyun Leng [a], Haitao Lu [a], Rongyu Xu [a], Yanping Du [b], Qi Li [a,*], Yuting Wu [a]

[a] MOE Key Laboratory of Enhanced Heat Transfer and Energy Conservation, Beijing Key Laboratory of Heat Transfer and Energy Conversion, Beijing University of Technology, Beijing, 100124, China

[b] Department of Engineering, Faculty of Environment, Science and Economy, University of Exeter, Penryn Campus, Penryn, Cornwall TR109FE, UK

*Corresponding author: liqi@bjut.edu.cn;

Abstract

This work concerns the fabrication of a salt based form-stable phase change composite by employing halloysite nanotube (HNT) as ceramic supporting material (CSM). The HNT has been broadly reported for preparation of low-temperature organic composites but very little has been done in medium and high temperature thermal energy storage fields. Herein we demonstrate for the first time with the use of HNT as skeleton substance for the fabrication of salt composite by cold compression and hot sintering technology. The feasibility of material fabrication is confirmed by evaluating a case containing a salt of sodium nitrate as phase change material and HNT as CSM. The effect of preheating treatment of HNT on the microstructure and phase change behaviours as well as cycling performance of the composite are is investigated. The results show that HNT can be wetted by the liquid nitrate salt at elevated temperatures, verifying the viability of the present strategy by using HNT as SSM for the synthesis of salt composite. A stable chemical structure is achieved in the salt-HNT composite, which confirms a preeminent chemical stability and compatibility between the HNT and nitrate salt. The hollow tubular structure of HNT could not only be able to provide extra surface for accommodating liquid salt to form a dense composite, but also strengthen the thermal stability of the nitrate salt. The preheating treatment of HNT at 300 °C and 500 °C respectively causes the occurrence of dehydration and dehydroxylation process, which in turn leads to the morphology and microstructure change of HNT, and hence affects the cycling performance of the composite. In comparison with the composite made from HNT preheated at 500 °C where a serious pulverization and deformation has been observed after 100 thermal cycles, the composite containing HNT preheated at 300 °C presents more stable structure and excellent cycling performance, revealing that the HNT is only suitable for the accommodation of inorganic salt that having application temperature limit less than 500 °C.

Keywords: Composite phase change materials; Halloysite nanotubes; Shape stability; Thermal energy storage; Medium and high temperature

1. Introduction

Thermal energy storage (TES) technology refers to the collection of excess heat or cold energy in virtue of a so-called storage medium and making use of them through energy conversion processes, and has been demonstrated to be one of the most potent ways to eliminate the energy mismatch between supply and demand [1-3]. Among the three TES technologies of sensible heat thermal storage, latent heat thermal storage and thermochemical heat thermal storage, the phase change material (PCM) based latent heat storage manner has drawn wide attentions in last decades due to the merits of isothermal melting and freezing processes, large heat storage capacity and rational investment outlays [4-6], and exhibited a multitude of potential applications in thermal energy storage fields such as cold chain logistics transport, building energy efficient heating and load shifting of energy networks [7, 8].

Owing to the advantages of applicable phase transition point, good thermal stabilization, and high latent heat as well as reasonable cost, molten salt has been widely employed as PCMs and utilized in medium-high temperature fields [6, 9-11]. Restricted by the two main issues of high temperature corrosion and poor thermal conductivity, however, the wide-scale use of these salt based materials has been restricted to some extent. Recent researches have revealed that the fabrication of shape-stabilized phase change composite presents solution to overcome these barriers [6, 8, 10]. In such salt composites, a ceramic supporting material (CSM) for shape stability and a highly conductive additive (HCA) for performance enhancement are typically involved. The combination of these ingredients by using either a cold compression-hot sintering or cold sintering fabrication approach could not only achieve a compact structure that is able to adsorb the liquid phase of salt and avoid the divulgence, but also endow the composite with excellent mechanical and thermophysical properties [12, 13]. Zhang et al. [14, 15] fabricated a solar salt based composite by using silicon carbide porous foam as CSM and indicated that the temperature distribution in the composite was more uniform compared with the pure salt because of the larger thermal conductivity in the composite than the pure salt. Liu et al. [16] evaluated a nitrate salt composite based on anorthite and cordierite ceramics. It was reported that anorthite ceramic presented better thermal stability than cordierite ceramic, while the latter ceramic was better than the former one for thermal conductivity enhancement. Anagnostopoulos et al. [17, 18] reported a salt based composite by employing red mud as CSM and it was indicated that the composite had good chemical compatibility and thermal stability in which an average thermal conductivity of 0.8 W/m·K and heat storage capacity of 1390 MJ/m^3 can be achieved. With the use of a porous Si_3N_4 ceramic as CSM, Wang et al. [19] investigated a ternary chloride salt composite and they found that the porous ceramic could also be able to act heat transfer enhancer apart from structure supporting substance. Compared to the pure salt, the melting rate in the composite can be strengthened by more than six times. Liu et al. [20] investigated a chloride salt-expanded graphite composite and revealed that more than 85% salt can be involved in the composite and in such a composition, a melting latent heat over 161 J/g and solidifying heat over 160 J/g can be achieved.

Apart from the above mentioned skeleton substances, some other ceramics or porous media such as MgO [21], graphite foam [22], vermiculite [23] and diatomite [24] have also been reported to be used as CSM for salt based composites fabrication. Halloysite nanotube (HNT) as an aluminosilicate clay having an Al:Si ratio of 1:1 that chemically similar to kaolin could also be a promising

candidate for preparing salt composite [25-27]. Such substance presents a hollow nanotubular structure and hence offers large surface area that be able to effectively encapsulate the liquid salt during phase transition process. Several investigations have been performed to use HNT as an adsorbent for organic composite fabrication [28-31], however, no work has been reported by utilizing such clay to prepare salt composite for medium-high temperature applications. This form the main motivation of this work, in which a shape-stable salt composite with the use of HNT as CSM and sodium nitrate as PCM for the first time is synthesized and investigated by a cold compression-hot sintering technology. It was reported that the water molecules on the inner surface of HNT will be eliminated at a heat treatment environment of 300 °C, leading to the layer distance of this multilayer tubular structure changed from 10 Å to 7 Å [27]. At a temperature range of 400-500 °C, the dehydroxylation happens, and due to the removal of hydroxyl groups, amorphous structure will be generated since part of the crystalline structure will be transformed into an amorphous one. Such structure change of HNT will make an impact on the composite structure formation and stabilization. Therefore, the effect of preheating treatment of HNT on the composite microstructural characteristics and thermophysical properties is evaluated. More specifically, the heat treatment is first conducted to confirm the structural variation and obtain different structured HNT by heating the ceramic at a temperature of 300-500 °C. The feasibility of material fabrication is then demonstrated by evaluating the wettability between the salt and HNT that experienced different preheating temperatures. Finally, the effect of thermal treatment of HNT on the microstructure and phase change behaviours as well as cycling performance of the composite are is investigated. The results obtained in this work provides guidance for using of HNT to fabricate salt composite and also enriches the research on the development of shape-stabilized composite for medium-high temperature thermal energy storage applications.

2. Materials and method

2.1. Raw materials

The analytically pure sodium nitrate with a melting point round 306 °C (NaNO3, purity > 99.9%, Beijing Yi-Li Chemical Co., Ltd, China) was used for the composite fabrication. HNT with a purity of 95% that got from Sigma-Aldrich Co. LLC, USA was employed as CSM. These two materials were used as purchased with no further purification.

2.2. Preparation of salt/HNT composites

A cold compression and hot sintering approach was used to fabricate the $NaNO_3$/HNT composite. Fig. 1 shows the fabrication procedure and more details for such a method can reference our previous investigations [7, 11]. In this study, the preparation process for the HNT-$NaNO_3$ composite can be divided into the following three steps. Step 1 was to accurately weigh the ingredients of $NaNO_3$ and HNT with a desired mass ratio in a balance, following followed by transporting these two materials into a stainless steel crucible and mixing the sample in a milling jar of a Planetary Mill Pulverisette (Fritsch, UK) at a speed of 200 rpm for 30 min. To investigate the effect of preheating treatment of HNT on the composite microstructure and thermal properties, the HNT was respectively preheated at a temperature of 300 °C and 500 °C for 10 hours prior to the material profiling. Step 2 was to shape the particle mixture into disk-like module with 12.5 mm in diameter

and 5 mm in thickness using a uniaxial press by a pressure of 100 MPa for 10 min to achieve green composite pellet. Step 3 was to sinter such green pellets in an electric heating furnace with the use of the following temperature program: heating from room temperature to 120 °C with a rate of 2 °C/min, and holding at 120 °C for 30 min to eliminate the absorbed water; then heating further to 320 °C at a rate of 5 °C/min, and maintaining for 50 min; and finally cooling the sample by using a reversed temperature programme to the heating process. By changing the mass concentration of $NaNO_3$ and HNT, and repeating the above fabrication steps, a variety of composites containing different compositions can be achieved.

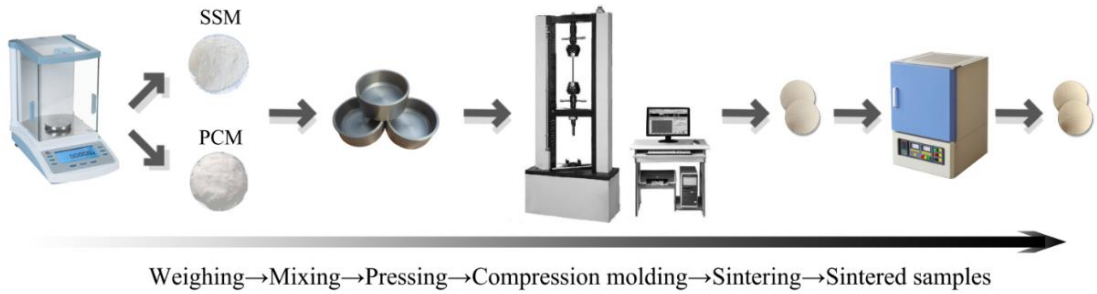

Fig. 1. Fabrication process for the salt-HNT composite with the use of cold compression and hot sintering approach.

2.3. Characterizations

Wettability measurement was performed by using a contact angle/surface tension meter (Dataphysics DCAT21, Germany). The chemical structure and compatibility were evaluated by a Fourier transformation infrared spectrometer (FT-IR, TENSOR 27, BURKER, Germany) with the spectrum from 400-4000 cm^{-1} and an X-ray diffraction (XRD, D8, BURKER, Germany) with a scanning angle over 10-90° and a step interval of 0.02°. The microstructural and morphological characteristics were analysed by a scanning electron microscope coupled with an energy dispersive X-ray spectroscopy detector (SEM-EDS, S4800, HITACHI, Japan). The phase change behaviours of the composite including melting point, latent heat and heat capacity were characterized by a Simultaneous Thermal Analyser (STA 449F3, Netzsch, Germany). The thermal stability was measured using a thermogravimetric analyser (TGA, Perkin Elmer Co. Ltd., Waltham, MA, USA). The thermal cycling performance was studied by using a self-built installation containing a high-temperature and a low-temperature chambers covering a temperature range of 25-1500 °C. A heating and cooling rate of 10 °C/min was selected for experiments, and a thermocouple inserted into the composite was used for monitor the composite temperature and control the thermal cycling.

3. Results and discussions

3.1. Microstructure change of HNT and optimal composition in the composite

As mentioned above, the heat treatment will lead to the microstructure change of HNT. To reveal the effect of treatment temperature on the microstructure, the TG and XRD analyses on the HNT

samples are carried out prior to the confirmation of optimal composition in the composite. For doing so, the HNTs are respectively preheating treated in an electrical heating furnace (KJ-M1200-12LZ, Zhengzhou Kejia Electric Furnace Co., Ltd, China) at temperatures of 300 °C and 500 °C. Fig. 2 (a) shows the TG curve for the HNT that experienced different treatment temperature. One can see three stages of weight loss apparent: the stage I is the normal temperature section; the stage II is the complete transformation of the layer spacing from 10Å to 7Å at a heat treatment temperature of 300 °C for 10 hours; the stage III is the dehydroxylation section after heat treatment at 500 °C for 10 hours. During this stage, a change in the crystal structure is occurred. Fig. 2 (b) illustrates the XRD results for these three-stage samples. Because stage II is only a complete water loss process compared to stage I, it can be seen that the XRD curves of the stages I and II tend to be the similar. However, in stage III, the characteristic peak of Al-OH is disappeared due to the transformation of the crystalline structure. This confirms the microstructure change of HNT after heat treatment at 500 °C in comparison with the sample treated at 300 °C. To further demonstrate this variation, the microstructures of these three-stage HNTS are observed and the results are illustrated in Fig. 2 (c-e). One can see that all HNTs present hollow tube structure, and this tubular characteristic endows them with the capacity to be a good adsorption carrier and skeleton substance. HNTs at stage II of are characteristic of larger lumen and slimmer tube shape compared to the that at stage I. This may be due to the reduction in layer spacing caused by dehydration. Compared with the HNTs at stages I and II, the structure of HNT at stage III becomes relatively loose and fragile, and the lumen seems to be enlarged. This is that for a given high temperature condition, breakage of the ionic bond connecting Al-OH leads to dihydroxylation.

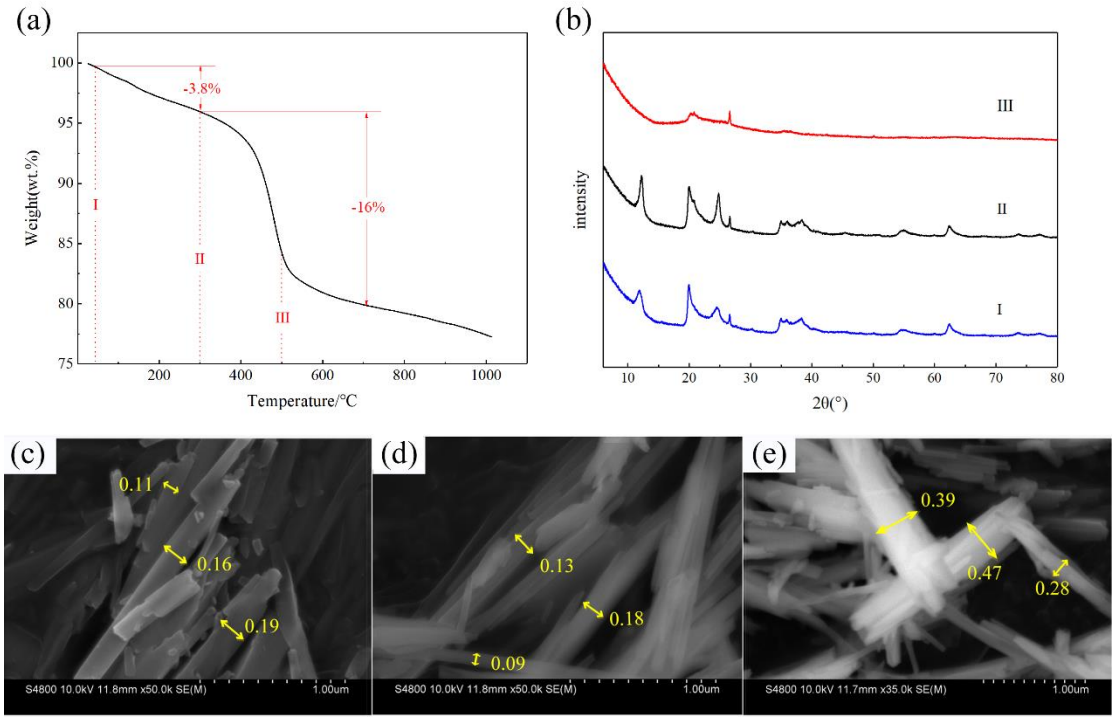

Fig. 2. (a) TG curves of HNT (b) XRD curves of HNT at stages I, II and III (c) SEM picture of HNT at stage I (d) SEM picture of HNT at stage II (e) SEM picture of HNT at stage III.

To further seek out the effect of preheating treatment of HNT on the composite microstructure and formation, three types of samples containing different staged HNTs are prepared and investigated.

Namely, mixed the salt with different concentration of HNTs, varied composites having mass ratios of 4:6, 5:5, 6:4, 7:3 and 8:2 can be obtained. The CPCMs are respectively named as CPCM-I, CPCM-II, CPCM-III, which corresponds to the three-stage HNTs that experienced different treatment temperatures. A visual leakage inspection is then carried out to confirm the optimal composition between the salt and HNT in the composite. Fig. 3 shows the appearances of these three CPCMs before and after sintering. It can be observed that after sintering, CPCM-I starts to exhibit less leakage and little deformation at a mass ratio of 5:5, and bulge at a mass ratio of 7:3 with severe salt leakage and shape deformation occurred at a mass ratio of 8:2. The salt accommodation capacity of CPCM-II has been improved compared to CPCM-I, which presents less leakage at a mass ratio of 6:4 although serious leakage and deformation has also been observed at a mass ratio of 8:2. The salt loading capacity of CPCM-III has a small difference relative to the CPCM-II, but a slight depression occurs at a mass ratio of 8:2. The detailed leakage examination results can be found in Table 1. Considering the obvious appearance difference among these three composites, and also the fact that the thermal cycling temperature of 320 °C is close to the heat treatment temperature of stage II, only the samples of CPCM-II and CPCM-III that made from the HNTs after medium and high temperature treatment are chosen for the further comparison, in which the mass ratio of 5:5 is selected for ensuring excellent shape stability.

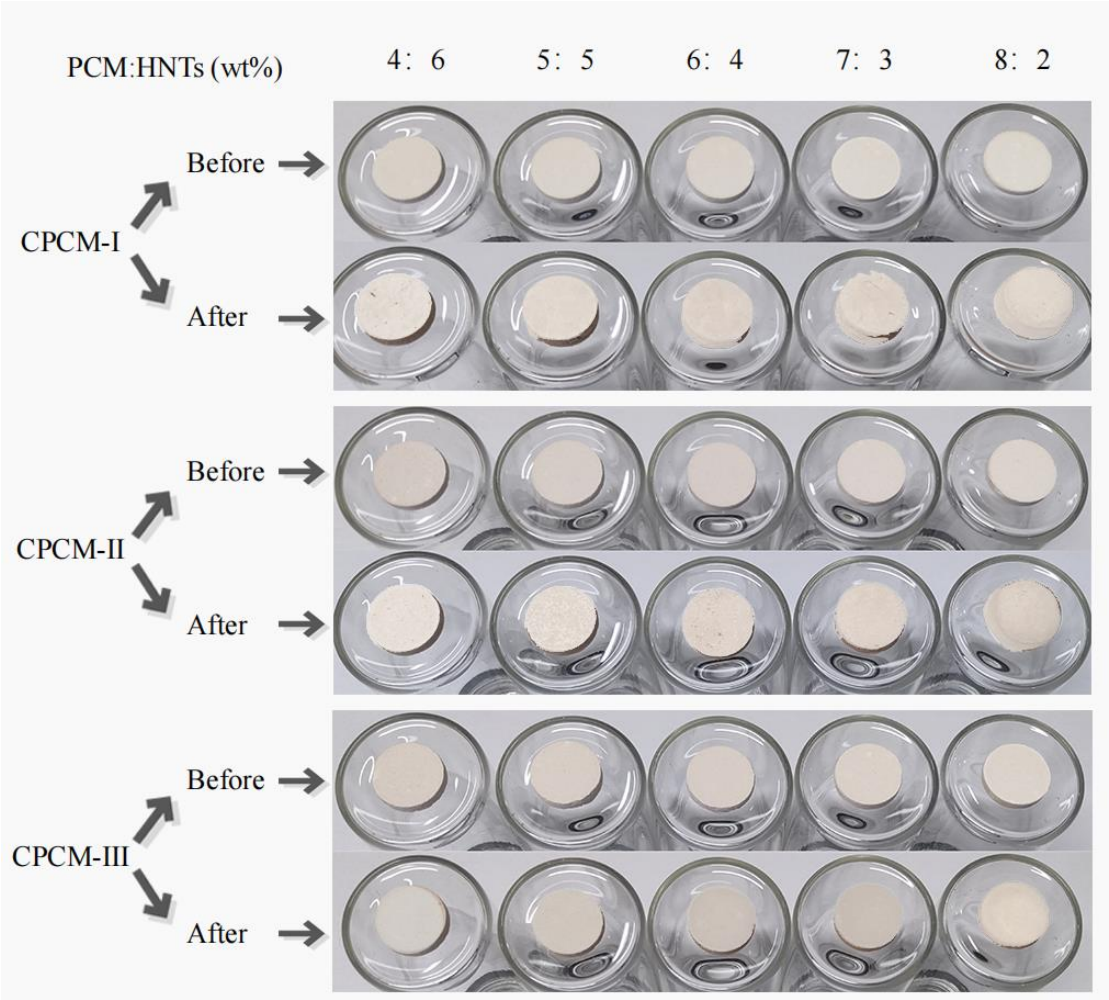

Fig. 3. Appearance of CPCM-I, CPCM-II and CPCM-III before and after sintering.

Table 1 Leakage inspection of CPCM-I, CPCM-II and CPCM-III before and after sintering.

Mixing cases (Salt-HNT)	4:6	5:5	6:4	7:3	8:2
Leakage (CPCM-I)	●	▲	▲	■	■
Leakage (CPCM-II)	●	●	▲	▲	■
Leakage (CPCM-III)	●	●	▲	▲	■

● Indicates that the sample has no deformation, leakage and excellent appearance; ▲ Indicates that the sample has less leakage and little deformation; ■ Indicates that the sample has large leakage and severe deformation

3.2. Wettability analysis between the salt and HNTs

For comparing the absorption ability of HNT on the salt, the wettability between the salt and HNT is evaluated in this section by measuring their contact angle in a high temperature surface tension analyser. In a typical salt composite, the skeleton substance is used for holding the liquid salt and maintaining the composite structure stabilization, which is generally demanded to have splendid interfacial energy that could be easily wetted by the liquid salt when the operation temperature surpasses its melting point [11]. For HNT used in this work, the microstructure change induced by high temperature treatment will affect its wettability with liquid salt. To investigate this, the wettability of liquid salt on the different-stage HNTs is measured and analysed. According to Young's equation, the contact angle between the salt and HNT can be calculated as follows [7]:

$$cos\theta = \frac{\sigma_{sv(HNT)} - \sigma_{sl(HNT/salt)}}{\sigma_{lv(salt)}} \quad (1)$$

where σ_{sv} and σ_{lv} denote the solid/vapour and solid/vapour interfacial energies, respectively, σ_{sl} stands for the interfacial energy of solid/liquid phase. In a typical experiment, a desired mass of salt is shaped into a cylindrical configuration before putting onto the substrate that made from HNT particles, followed by transporting the salt/HNT sample into the observation chamber. A high-resolution video camera combined with drop image processing software is used for filming the contact angle image and obtaining the result. For comparison purpose, one surface of these two-stage HNT substrates is burnished by using 400-, 2000- and 5000-grit sandpaper to achieve the same roughness. First, the contact angle variation between the liquid salt and HNTs over a temperature range of 300-400°C is investigated. Fig. 4 plots the measurement results. One can see that for both substrates, the contact angle gradually decreases with the increase of operating temperature, and the measured values are respectively 74.3° and 59.5° for these two substrates at 400 °C. This indicates that the salt has outstanding wettability with HNTs, and HNTs after medium and high temperature heat treatment have the potential to be used as skeleton material for the salt composite fabrication. An observation of Fig. 4 also indicates that the HNT at stage-III achieves smaller contact angle with salt than that at stage-II at a measurement temperature of 400 °C, and the contact angel variation rate of stage-III HNT is more quickly than that of stage-II HNT. The reason for such an observation may be attributed to that after the high temperature treatment, the ionic bond activity connecting Al-OH in the stage-III HNT becomes active and its hollow structure presents characteristics such as

larger lumen, fragility and looseness. This leads to more difficulties in densification and hence more micropores exist on its surface and also the penetration of salt is increased during measurement process.

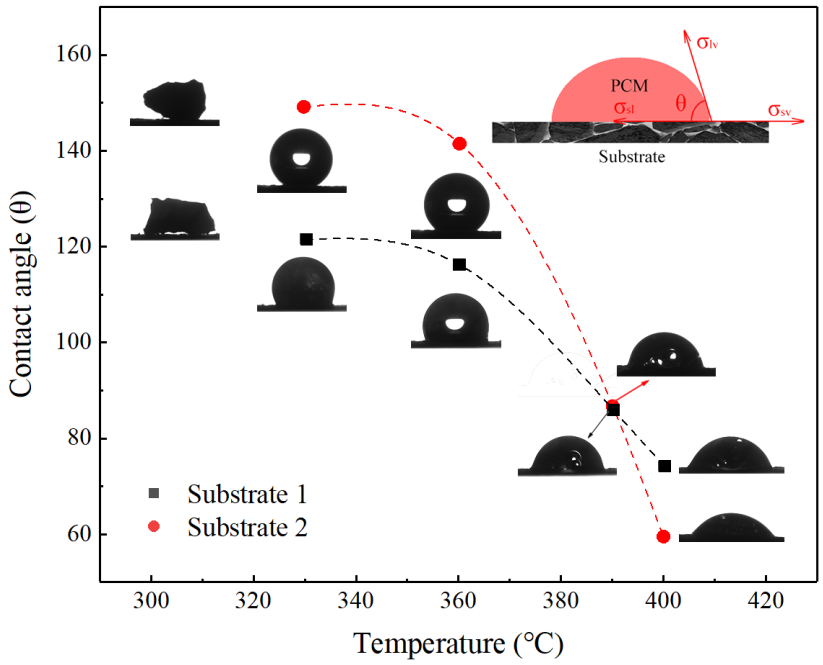

Fig. 4. Contact angle measurements of liquid salt on the HNTs as a function of operating temperature. Substrate 1 indicates the HNT preheated at 300 °C and Substrate 2 denotes the HNT preheated at 500 °C.

The variation of contact angle increments of liquid salt on the HNT substrate with time is then analysed and the data is reprocessed in Fig. 5. It can be observed that for both substrates, the contact angle changes with time and the variation is consisted of three stages. Stage (1) is the initial stage, during which the contact angle changes very little and the salt is in short-term balance with substrates 1 and 2 at the beginning of the melting. Stage (2) is a spreading stage at which the molten salt is affected by the adsorption of substrates 1 and 2. During this stage, salt spread on the substrate and penetration into the substrate occur, leading to a sharp variation of contact angle measurement value. Stage (3) is a stable stage, during which the liquid salt on the HNTs substrate reaches a stage of energy balance since the contact surface and micropores are fully filled by the liquid salt. From Fig. 5, it can be also found that there exists a large difference in the evolution of the contact angle of salt on different HNT substrate, with a difference of 1° in the contact angle reduction, and the contact angle reduction rate of salt on substrate 2 is faster. This is due to the structural differences of HNTs after medium and high temperature heat treatment. Substrate 2 has larger cavities and hollow tubes are loose and disordered, making it more difficult to densify, and the pressed substrate has stronger adsorption and more micropores, so it performs better in terms of wettability. This result, integrated with the observations illustrated in Figs. 3 and 4, demonstrate that the HNTs can be wetted by the liquid nitrate salt at elevated temperatures, at which the HNT experienced a treatment temperature of 300 °C achieves a superior wettability than that experienced a heat

treatment of 500 °C.

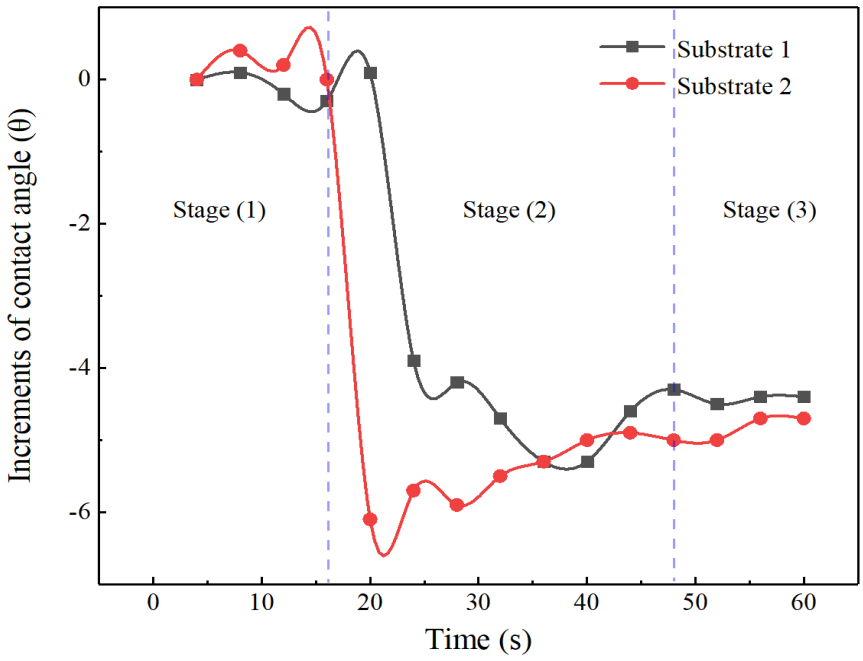

Fig. 5. Variation of contact angle increment of liquid salt on HNTs with time. Substrate 1 indicates the HNT preheated at 300 °C and Substrate 2 denotes the HNT preheated at 500 °C.

3.2. Chemical compatibility and physical stability of the composite

The chemical compatibility of the HNT based composite is evaluated in this section by measuring the XRD patterns at the ambient temperature. As plotted in Fig. 6, the results of salt, HNT and the composites experienced thermal cycles are included for comparative analysis. One can see that the main characteristic peaks for pure nitrate salt occur at 2θ=29.3°, 31.7°, 38.9°, 47.9° (Fig. 6 (a)), which is consistent with the result reported by [32]. For HNT after preheating treated by a temperature of 300 °C, a broadened asymmetric peak is observed, as illustrated in Fig. 6 (b). This is mainly due to the curved crystal lattice of kaolinite [27]. With the increase of thermal treatment temperature from 300 °C to 500 °C, the peak is disappeared and becomes smooth because the transformation of the crystalline structure. For the composite containing salt and HNT, only the peaks similar to that of the pure salt and HNT are apparent and no new peak is observed, as indicated in Figs. 6 (c) and (d). This reveals that no chemical reaction is occurred between the salt and HNT, and a preeminent chemical stability has been generated in the composite after experienced fabrication process. By comparing the XRD results of the composites that sustained different heating-cooling cycles (Figs. 6 (e) and (f)), it can be found that all peaks are identical to that in the individual ingredients of salt and HNT, and also the sintered composite. This further demonstrates that no new chemical bonds are created over the repeated thermal cycles, and the HNTs are chemically compatible with the salt even at high operation temperature.

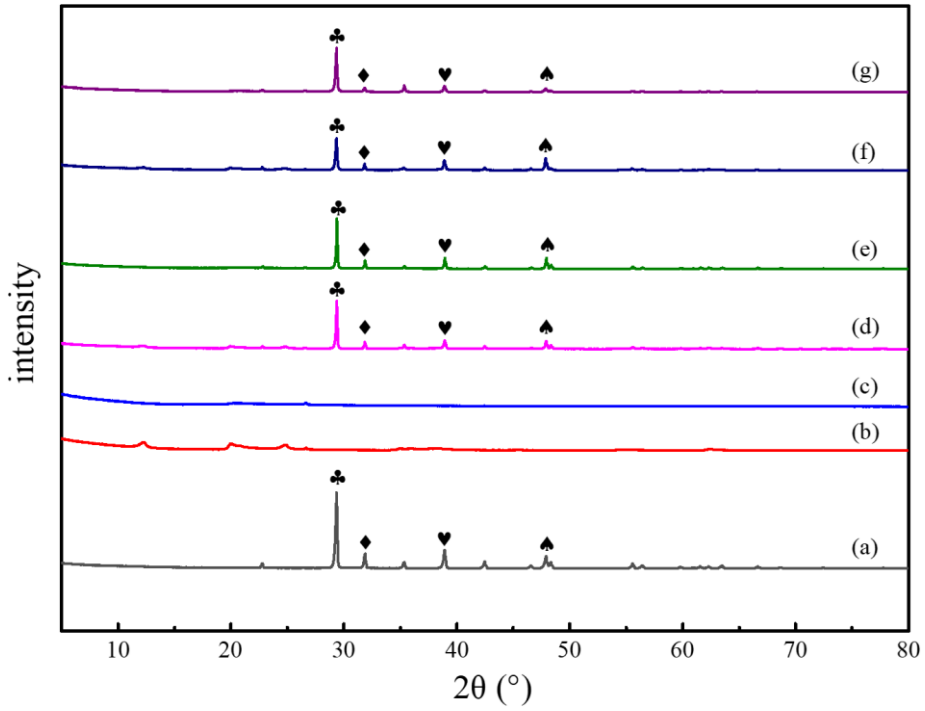

Fig. 6. XRD patterns of the (a) pure salt, (b) HNT after treated at 300 °C, (c) HNT after treated at 500 °C, (d) salt-HNT composite (300 °C), (e) salt-HNT composite (500 °C), and (f) and (g) composite experienced 100 thermal cycles.

To further determine the chemical and physical compatibility of the salt-HNT composite, the FT-IR analysis is also carried out. Fig. 7 illustrates the measurement results. It is seen that three apparent peaks of 833 cm^{-1}, 1390 cm^{-1} and 2431 cm^{-1} are apparent for the pure nitrate salt (Fig. 7 (a)). The first absorption peak is induced by the N-O symmetric stretching vibration, while the latter two peaks are mainly caused by the N-O stretching vibration [6]. As for the HNT treated at 300 °C, two main peaks of 3623 cm^{-1} and 3696 cm^{-1}, and several small peaks below 1100 cm^{-1} are observed (Fig. 7 (b)). The 1033 cm^{-1} peak is assigned to the stretching vibrations of Si-O-Si, while the peaks of 3696 cm^{-1} and 3623 cm^{-1} are related to the Al-OH structure [29]. Raising the thermal treatment temperature from 300 °C to 500 °C, these distinct absorption peaks are disappeared in the HNT, as exhibited in Fig. 7 (c). This is due to the occurrence of dehydroxylation and the transformation of the crystalline structure. Such observations also verify the breakage of the Al-OH ionic bond in HNT over the heat treatment process. Fig. 7 (d) and (e) plots the measured results for the salt-HNT composite. One can see that no additional spectrum peaks are emerged apart from the absorption characteristics of the salt and HNT. Shown in Fig. 7 (f) and (g) are the patterns of the composites experienced 100 thermal cycles and it is seen that two similar curves that combined the peaks of salt and HNT are achieved. These observations indicate that no new chemical bonds are generated in the composite and the salt and HNT are physical stability.

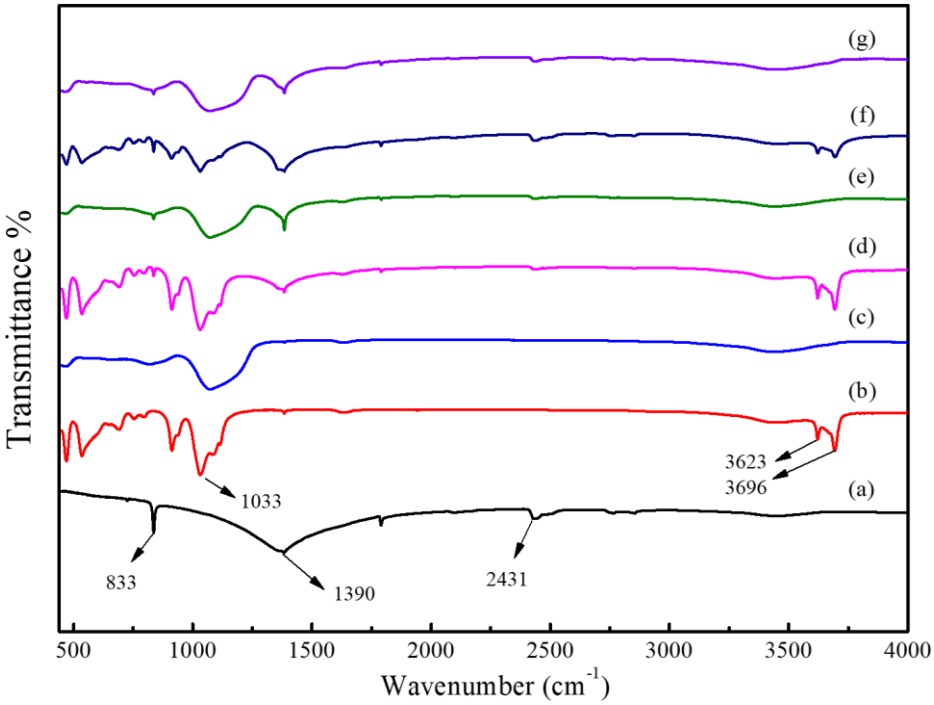

Fig. 7. FT-IR spectra of the (a) pure salt, (b) HNT after treated at 300 °C, (c) HNT after treated at 500 °C, (d) CPCM-II after one thermal cycle, (e) CPCM-III after one thermal cycle, (f) CPCM-II after 100 thermal cycles, and (g) CPCM-III after 100 thermal cycles.

3.3. Microstructure analysis and morphological characterization of the composite

Fig. 8 illustrates SEM observations of the salt based composites made by different preheating treatment temperature of HNTs. One can see that for both composites, a homogenous distribution of the salt and HNT has been achieved in the observation area with the tubular configuration of HNT being clearly identified. The high wettability of HNT can hold the liquid salt and forms a dense composite structure that could be able to effectually restrict the leakage during the repeated thermal cycles. From Fig. 8, it can also be seen that a molten salt liquefied structure is generated in both composites. This observation is consistent with our previous investigations [9] and also the work reported by Ge et al. [33]. In the salt-HNT composite, the physical blending and configuration shaping enable a uniform distribution of salt and HNT, and an increased composite density over the sample fabrication process. During sintering, the salt melts and changes the phase state from solid to liquid. In such a process, the microscaled movement of liquid salt in the confined area occurs to form the molten salt liquefied structure, which pull the migration of skeleton substance moving together and lead to the occurrence of particle rearrangement within the composite. Consequently, the composite structure can be further intensified and compacted. Due to the high wettability of skeleton ceramic towards the salt, the liquid salt can be efficaciously encapsulated by the ceramic material and accommodated within the composite. Compared to other traditional ceramics, the hollow tubular structure of the HNT provides relatively large surface for contacting the liquid salt and hence an enhanced ability for retaining the salt and preventing liquid phase leakage can be achieved.

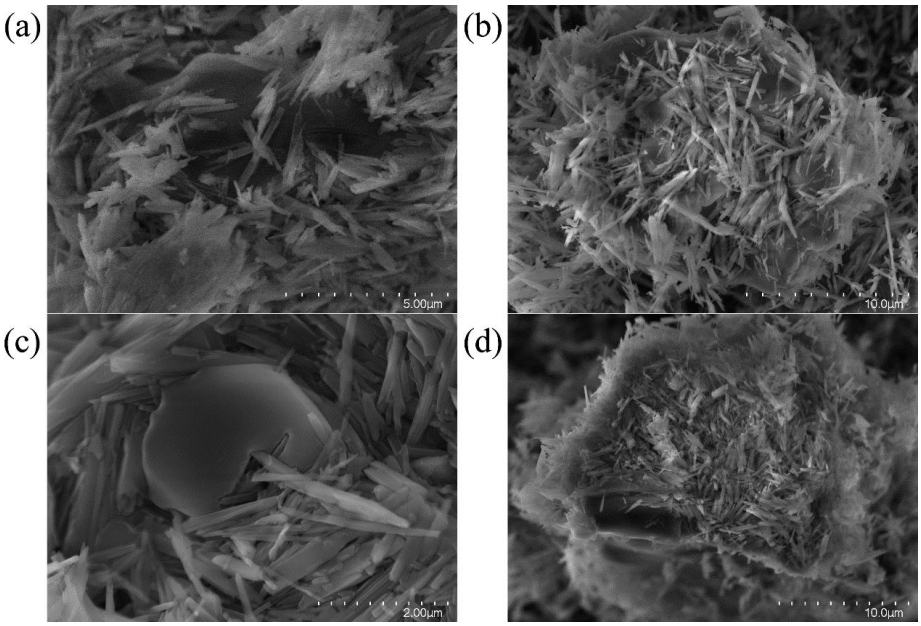

Fig. 8. (a) CPCM-II before sintering, (b) CPCM-II after sintering, (c) CPCM-III before sintering, and (d) CPCM-III after sintering.

Fig. 9 shows the EDS mapping results for the salt-HNT composite. In this analysis, an identical observation area from the composite is selected for investigating and the elements of Na and N are used for indicating the distribution of salt in the composite. One can see that the salt is equably distributed in the observation area after the sample experienced one thermal cycle. With the evolvement of thermal cycling process, the element concentrations of Na and N seem to be decreased but the distribution becomes more uniform in the observation region. This is because that the thermal cycling will cause the structure and ingredient redistribution in the composite [9, 33]. For a salt based composite experienced repeated heating-cooling cycles, the movement of liquid salt within the microcavities and micropores leads to the migration of ceramic particles. This microscopic motion in turn achieves a more even distribution of ingredients and hence an element variation presented in Fig. 9.

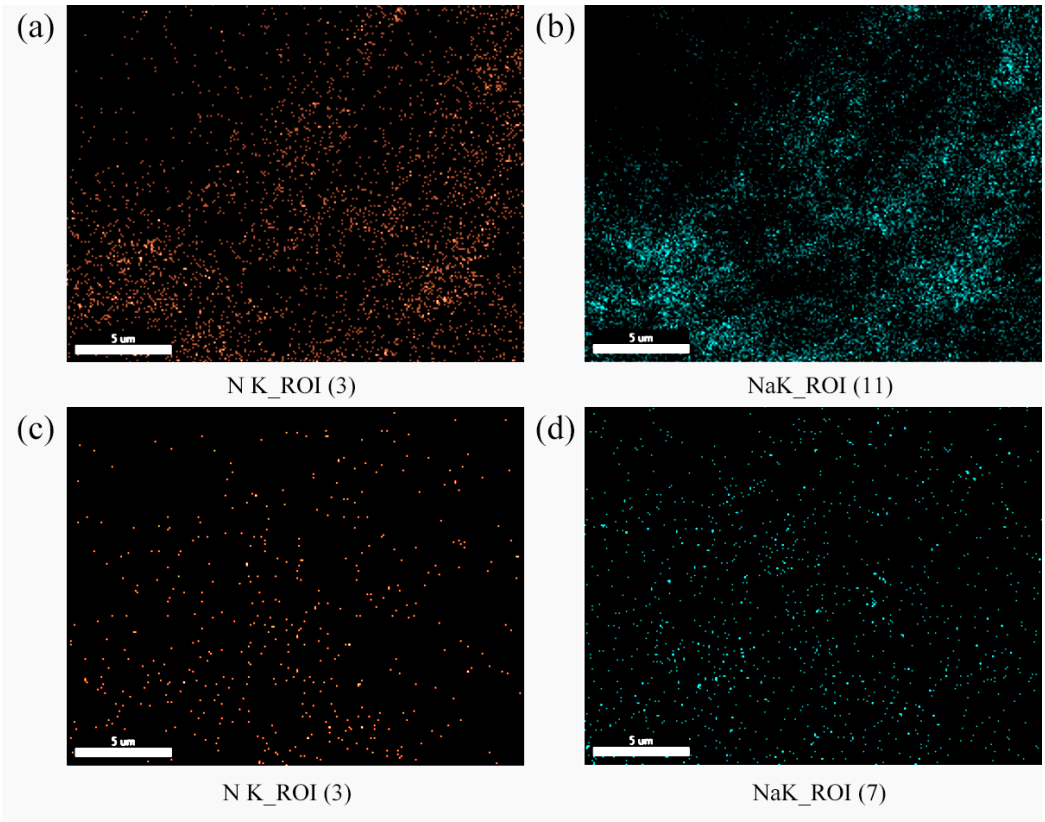

Fig. 9. EDS element maps in the composite. (a) and (b) after one thermal cycle, and (c) and (d) after 100 thermal cycles.

3.4. Phase change behaviours of the composite

The DSC measurements for the pure salt and salt based composites are illustrated in Fig. 10. In this analysis, the composite containing a mass ratio of salt:HNT=5:5 is prepared and investigated. It can be seen that two endothermic peaks of a fuzzy one and a distinct one are observed for both the pure salt and salt composites. The first peak appears at a temperature range of 250-280 ℃ and represents the occurrence of solid-solid phase change of nitrate sodium, while the second peak indicates the solid-liquid phase transition that taking place at a temperature of 290-320 ℃. The temperature ranges for these two peaks at the two composites are almost the same, which are also accordance with the results presented in the pure salt. This indicates the mix of HNT with salt to fabricate composite has no effect on the phase change behaviour of salt. As for the measured latent heat, it is seen that the value for pure salt is around 170.38 J/g, while that of the two composites are respectively 85.33 J/g and 85.35 J/g. This is in agreement with the theoretical calculation that the composite latent heat should account for approximately 50% of the pure salt, which further verify that a good thermal stability between the salt and HNT has achieved in the composite. To estimate the latent heat storage and release ability of the salt-HNT composite developed in this study, a parameter of energy storage efficiency is employed for evaluation and the calculation formula can be written as follows [32]:

$$E_s = \frac{\Delta H_{s,com} + \Delta H_{m,com}}{\Delta H_{s,salt} + \Delta H_{m,salt}} \quad (1)$$

where $\Delta H_{s,com}$ and $\Delta H_{s,salt}$ are respectively the solidifying latent heats of the composite and pure salt, $\Delta H_{m,com}$ and $\Delta H_{m,salt}$ are respectively the melting latent heats of the composite and pure salt. Table 2 shows the detailed measurement results. Based on the measured values, the energy storage efficiencies for the two composites are 49.41% and 47.74%, which demonstrates that the fabricated composites respectively represent about 50% energy loading efficiency in comparison with the pure salt for a given identical mass.

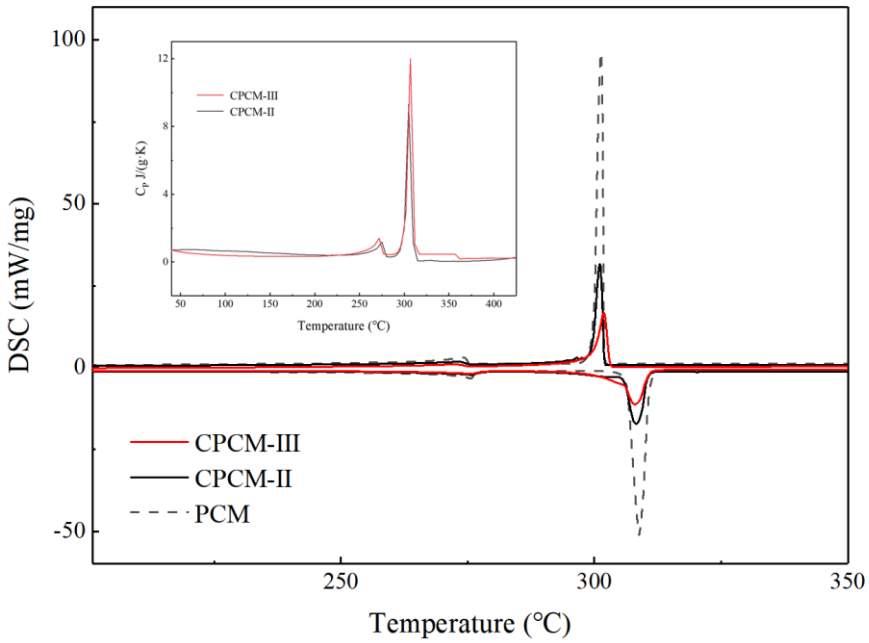

Fig. 10. DSC curves of PCM, CPCM-II and CPCM-III during both the charging and discharging processes. Insert is the heat capacity measurement result.

Table 2. Phase transition parameters of salt, CPCM-II and CPCM-III after the initial cycle

Sample	Melting			Freezing			Specific heat (J/g·°C)
	Onset (°C)	Endset (°C)	Latent heat (kJ/kg)	Onset (°C)	Endset (°C)	Latent heat (kJ/kg)	
PCM	305.97	310.46	170.38	302.44	300.57	168.13	0.65(s)/0.89(l)
CPCM-II	305.41	310.46	85.33	302.18	299.82	81.94	1.86(s)/2.84(l)
CPCM-III	304.94	310.99	85.35	303.53	300.23	76.26	1.42(s)/1.91(l)

It is mentioned above that a high heat treatment temperature will lead to the occurrence of the

dehydroxylation for HNT, it is meaningful to determine the maximum decomposition temperature of the composite. This is also one of the most significant properties for the utilization of composite in real applications. Fig. 11 depicts the TGA results for the pure salt and composites made by different HNTs. Prior to the experiments, all samples are placed in an electric drying chamber at 110 °C for 24 h to entirely exclude the effect of moisture. It can be seen from the figure that for pure salt, a two-step degradation on the weight loss is observed over the measuring temperature range, which is similar to the results presented by Yu et al. [32]. As for the salt-HNT composite, an apparent weight loss is exhibited particularly for the sample containing HNT that preheating treated at a temperature of 500 °C. Such weight variation is mainly caused by the dehydroxylation, which leads to the breakage of the ionic bonds of the Al-OH octahedra in their hollow structure. Ouyang et al. [27] has reported that the HNT will start to loss the absorbed interlayer water from room temperature to 200 °C. At a heat treatment temperature of 300 °C, there will be a complete loss of water molecules and inner-surface hydroxyl groups, causing the structure shrinkage and inter-layer distance reduction. When the temperature is further increased to 500 °C, the dehydroxylation process happens, leading to an apparent mass loss in this period. This is consistent with the observation presented in Fig. 11. It is demonstrated that the thermal decomposition temperature in a TGA curve can be regarded as the point at which 3% of weight loss has been taken place [21]. Correspondingly, the maximum operating temperatures for the pure salt and the two composites are respectively 593.1 °C, 614.2 °C and 615.6 °C. The composite decomposition temperature is higher than that the pure salt, which demonstrates the tubular structure of the HNT strengthens the thermal stability of salt. Fig. 11 also shows that there will be no weight loss for the salt-HNT composite when the operating temperature is around 550 °C. Considering that the composite phase transition temperature is about 305 °C, which is far less than the permitted safe temperature, it is therefore concluded that the salt-HNT composite developed in this work achieves excellent thermal reliability in medium and high temperature environments.

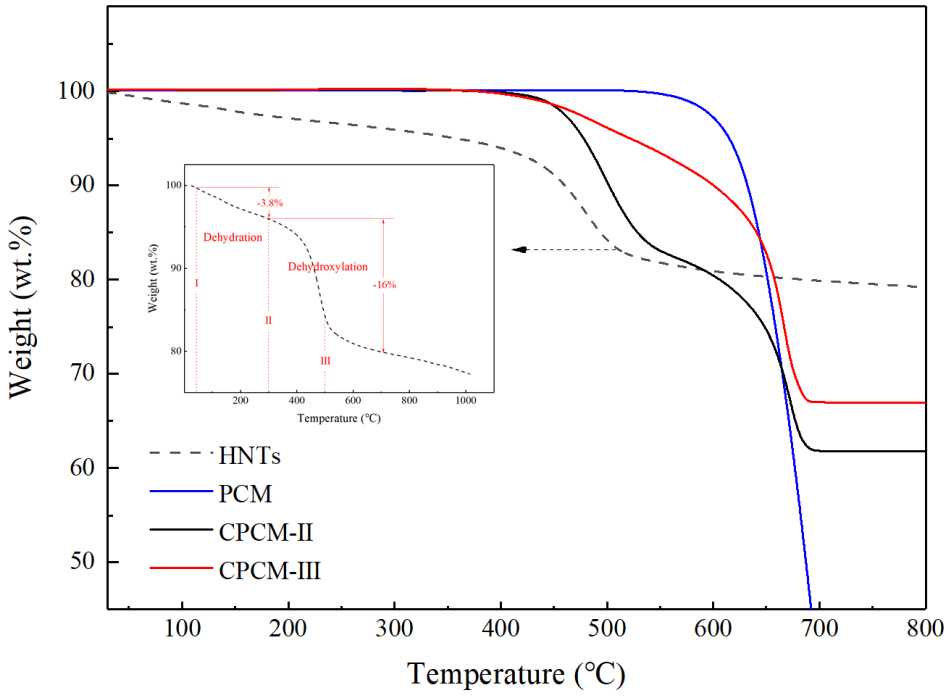

Fig. 11. TG curves of salt, CPCM-II and CPCM-III after the initial cycle.

3.5. Thermal energy storage and cycling performance of the composite

According to the parameters illustrated in Table 2, the composite heat storage capacity can be calculated. For a given temperature range, the heat storage ability can be obtained by using the following calculation equation [7]:

$$Q_e = \alpha \int_{T_0}^{T_s} C_h \, dT + \beta \left\{ \int_{T_0}^{T_m} C_{ms} \, dT + \Delta H_m + \int_{T_m}^{T_s} C_{ml} \, dT \right\} \quad (2)$$

where Q_e is the energy storage capacity; α and β are the mass fractions of HNT and salt, respectively; T_0, T_m and T_s are respectively the initial state temperature, phase change temperature and final state temperature, respectively; C_h, C_{ms} and C_{ml} are the specific heat capacities of HNT, solid state of salt and liquid state of salt; ΔH_m is the latent heat. Using the measured data summarized in Table 2, it can be calculated that the energy storage densities of CPCM-II and CPCM-III can respectively be reached up to 499.16 kJ/kg and 489.95 kJ/kg under a temperature of 30-500 °C. The calculated value in the composite containing HNT preheated at 300 °C is higher than that in the composite containing HNT preheated at 500 °C, and both values are almost equal to that in the pure nitrate salt. The larger heat capacity of HNT than the nitrate salt could be a reason for this observation. The preheating treatment of HNT at different temperature could be another reason, which leads to the transformation of the crystalline structure of HNT and thereby a variation of measured specific heat capacity.

The cycling performance of the composite is estimated by heat treatment of samples under a temperature range of 50-320 °C. For doing this, the phase change behaviours of the composites after 50, 80 and 100 times of heating-cooling cycles are respectively analysed by DSC and the results are illustrated in Fig. 12. It is seen that three similar endothermal curves are observed for both two CPCMs, indicating that an excellent cycling performance seems to be achieved in these two composites. By comparing the detailed measured values of phase change temperature and latent heat, as summarized in Table 3, one can see that the phase transition point of the sample changes a little with the peak value being measured as around 306 °C. But for the latent heat, there is existence of stark difference between these two CPCMs. The measured value of latent heat in CPCM-II is decreased by only 1.7% after experienced 100 thermal cycles, while that in CPCM-III is a more than 9.9% reduction compared with the sample after one cycle. The reduction of latent heat occurred in CPCM-II is mainly due to the divulgence of salt in the repeated thermal cycles. In a salt-HNT composite, the incomplete accommodation of salt at the outer surface could occur the spillage and hence leads to the decrease of the latent heat.

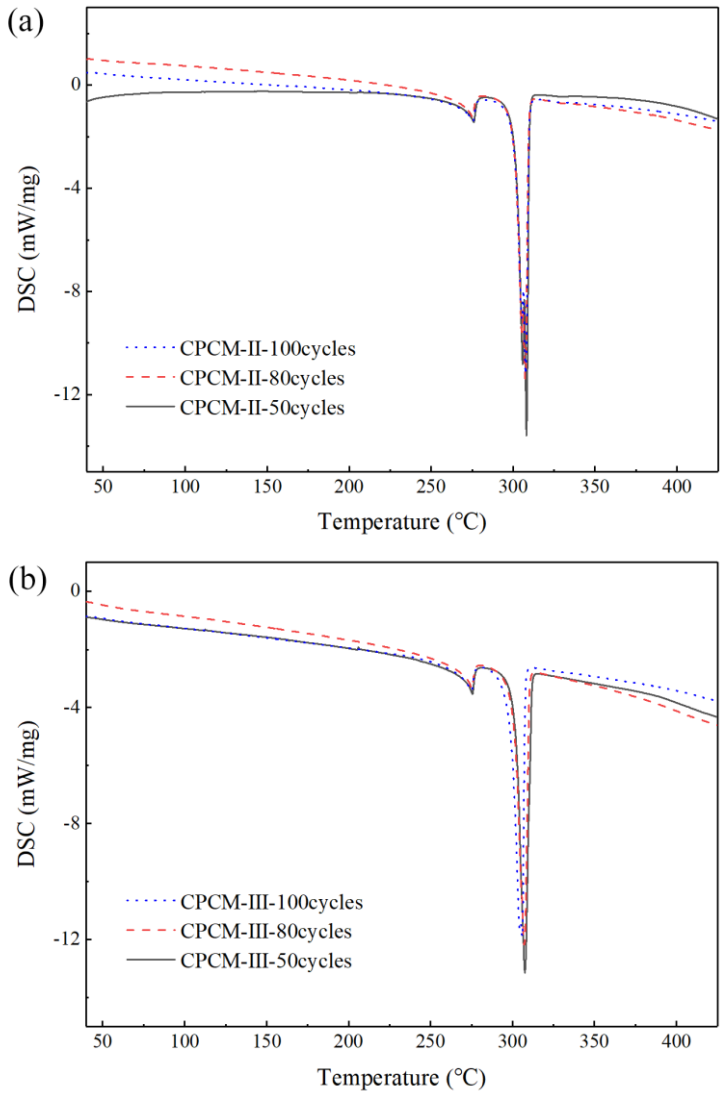

Fig. 12. DSC curves of CPCM-II(a) and CPCM-III(b) after 50,80,100 cycles.

Table 3. Phase change behaviours of CPCM-II and CPCM-III after different thermal cycles.

		Onset (℃)	Peak (℃)	Endset (℃)	Specific heat (J/g·℃)	Latent heat (kJ/kg)
50 cycles	CPCM-II	304.82	307.30	309.71	1.06(s)/0.82(l)	80.22
	CPCM-III	300.50	306.35	310.02	1.07(s)/1.43(l)	77.31
80 cycles	CPCM-II	302.86	306.49	309.24	1.43(s)/0.17(l)	79.44
	CPCM-III	301.40	306.66	310.84	0.93(s)/1.52(l)	73.73
100 cycles	CPCM-II	303.63	306.71	309.62	1.03(s)/3.12(l)	78.85
	CPCM-III	298.53	305.07	307.49	1.04(s)/1.33(l)	69.61

The variation of latent heat in CPCM-III could be associated with the structure deformation over the repeated thermal cycles. To verify this observation, the micro and macro morphology of these two composites after 100 cycles are evaluated and compared. Fig. 13 illustrates the observation results, and it is found that in comparison with CPCM-III where distinct pulverization and deformation has been exhibited, CPCM-II presents intact and stable shape with molten salt liquefied structure apparent in the observation area. Such a liquefied structure can efficaciously maintain the liquid salt and avoid the divulgence during cool-heat cycles. As analysed previously, the thermal treatment of HNT at 300 ℃ will fully remove the water molecules and internal surface hydroxyl groups, leading to the reduction of inter-layer distance and formation of a fine and close structure of HNT. The further heating of HNT to 500 ℃ will break the ionic bond in the Al-OH functional group and promote the dihydroxylation reaction. During such a process, its hollow tubular structure becomes fragile and loose, and forfeits the load ability to liquid salt. This observation together with the results presented in Fig. 11 further reveal that for using of HNT to fabricate composite utilized in medium and high temperature fields, it is suggested to accommodate salt at a suitable application temperature less than 500 °C since the high operating temperature could be able to induce the dehydroxylation of HNT and recede the composite cycling ability.

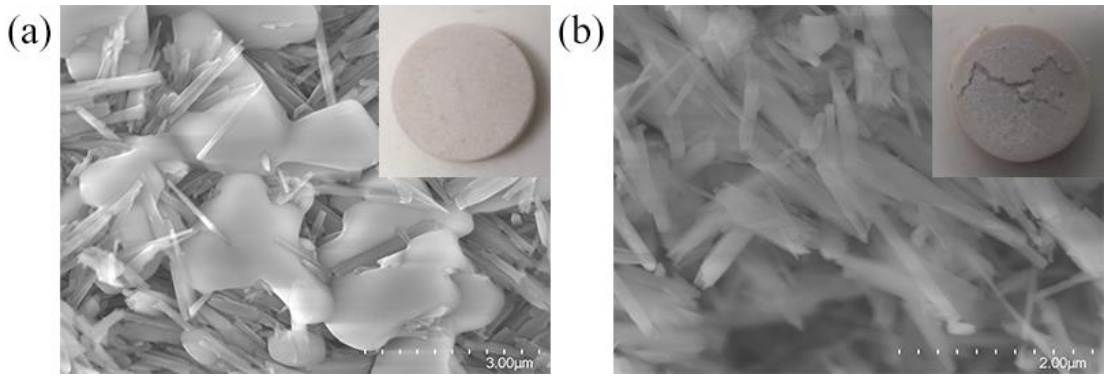

Fig. 13. Microscopic images of CPCM-II (a) and CPCM-III (b) after 100 cycles. Inserts are the macroscopic images of these two composites.

4. Conclusions

A shape stability salt based phase change composite containing halloysite nanotube as skeleton material is prepared and studied in this work. The feasibility of material fabrication by using of such ceramic as structure substance is demonstrated through evaluating a case with the use of the sodium nitrate as PCM. The effect of preheating treatment of HNT on the microstructure and phase change behaviours as well as cycling performance of the composite are analysed. The following conclusions can be obtained according to the investigations:

(1) The aluminosilicate clay of HNT can be wetted by the liquid nitrate salt at elevated temperatures, verifying the viability of the fabrication strategy by using HNT as skeleton substance for the synthesis of salt composite.

(2) A stable chemical structure is achieved in the salt-HNT composite, which confirms a preeminent chemical stability and compatibility between the HNT and nitrate salt. Moreover, the hollow tubular structure of HNT could not only be able to provide extra surface for accommodating liquid salt to

form a dense composite, but also strengthen the thermal stability of the nitrate salt.

(3) The preheating treatment of HNT at 300 °C and 500 °C respectively causes the occurrence of dehydration and dehydroxylation process, which in turn leads to the morphology and microstructure change of HNT, and hence affects the cycling performance of the composite.

(4) Compared to the composite made from HNT preheated at 500 °C where serious pulverization and deformation has been observed after 100 times of cool-heat cycles, the composite containing HNT preheated at 300 °C presents more stable structure and excellent cycling performance, revealing that the HNT is only suitable for the fabrication of salt composite that having application temperature limit less than 500 °C.

This work concerns only the feasibility of using HNT as skeleton substance for salt based composite fabrication and also the effect of preheating treatment of HNT on the microstructure and thermal properties of the composite. Investigation of performance enhancement of the composite by adding of highly thermal conductive enhancer is beyond the scope of this work but it is worth exploring nevertheless.

Acknowledgements

The work was supported by the Beijing Natural Science Foundation (3222026), and high-end talents development program, Carbon Neutral Foundation (049000514122611) and International Research Cooperation Seed Fund (Project No. 2021B40) of Beijing University of Technology.

References

[1] Fan-Yi Meng, I-Han Chen, Jiun-Yi Shen, Kai-Hsin Chang, Tai-Che Chou, Yi-An Chen, Yi-Ting Chen, Chi-Lin Chen, Pi-Tai Chou. A new approach exploiting thermally activated delayed fluorescence molecules to optimize solar thermal energy storage. Nature Communications 13 (2022) 797.

[2] Jason Woods, Allison Mahvi, Anurag Goyal, Eric Kozoubal, Adewale Odukomaiya, Roderick Jackson. Rate capability and Ragone plots for phase change thermal energy storage. Nature Energy 6 (2021) 295-302.

[3] Muhammad Tawalbeh, Hafsah A. Khan, Amani Al-Othman, Fares Almomani, Saniha Ajith. A comprehensive review on the recent advances in materials for thermal energy storage applications. International Journal of Thermofluids 18 (2023) 100326.

[4] Heng Gu, Yuanyuan Chen, Xiaoyan Yao, Li Huang, Deqiu Zou. Review on heat pump (HP) coupled with phase change material (PCM) for thermal energy storage. Chemical Engineering Journal 455 (2023) 140701.

[5] Tong Xiao, Long Geng, Yucheng Dai, Jiateng Zhao, Changhui Liu. UV-cured polymer aided phase change thermal energy storage: Preparation, mechanism and prospects. Journal of Energy Storage 64 (2023) 107066.

[6] Zeyang Kang, Sihan Huang, Xiangyang Liu, Ying Zhang, Maogang He. A novel high temperature eutectic salt and its composite with enhanced high conductivity. Journal of Energy

Storage 59 (2023) 106409.
[7] Qi Li, Lin Cong, Xusheng Zhang, Bo Dong, Boyang Zou, Zheng Du, Yaxuan Xiong, Chuan Li. Fabrication and thermal properties investigation of aluminium based composite phase change material for medium and high temperature thermal energy storage. Solar Energy Materials and Solar Cells 211 (2020) 110511.
[8] Zi-Rui Li, Nan Hu, Li-Wu Fan. Nanocomposite phase change materials for high-performance thermal energy storage: A critical review. Energy Storage Materials 55 (2023) 727-753.
[9] Chuan Li, Qi Li, Xuekun Lu, Ruihuan Ge, Yanping Du, Yaxuan Xiong. Inorganic salt based shape-stabilized composite phase change materials for medium and high temperature thermal energy storage: Ingredients selection, fabrication, microstructural characteristics and development, and applications. Journal of Energy Storage 55 (2022) 105252.
[10] Qing Wang, Chunlei Wu, Xinmin Wang, Shipeng Sun, Da Cui, Shuo Pan, Hongyu Sheng. A review of eutectic salts as phase change energy storage materials in the context of concentrated solar power. International Journal of Heat and Mass Transfer 205 (2023) 123904.
[11] Chuan Li, Qi Li, Lin Cong, Yongliang Li, Xianglei Liu, Yimin Xuan, Yulong Ding. Carbonate salt based composite phase change materials for medium and high temperature thermal energy storage: A microstructural study. Solar Energy Materials and Solar Cells 196 (2019) 25-35.
[12] Veerakumar Chinnasamy, Jaehyeok Heo, Sungyong Jung, Hoseong Lee, Honghyun Cho. Shape stabilized phase change materials based on different support structures for thermal energy storage applications-A review. Energy 262 (2023) 125463.
[13] K. Liu, Z.F. Yuan, H.X Zhao, C.H. Shi, F. Zhao. Properties and applications of shape-stabilized phase change energy storage materials based on porous material support-A review. Materials Today Sustainability 21 (2023) 100336.
[14] Shuai Zhang, Yuanpeng Yao, Yingai Jin, Zhen Shang, Yuying Yan. Heat transfer characteristics of ceramic foam/molten salt composite phase change material (CPCM) for medium-temperature thermal energy storage. International Journal of Heat and Mass Transfer 196 (2022) 123262.
[15] Shuai Zhang, Ziyuan Li, Yuanpeng Yao, Limei Tian, Yuying Yan. Heat transfer characteristics and compatibility of molten salt/ceramic porous composite phase change material. Nano Energy 100 (2022) 107476.
[16] Jicheng Liu, Jiamei Xu, Zijian Su, Yuanbo Zhang, Tao Jiang. Preparation and characterization of $NaNO_3$ shape-stabilized phase change materials (SS-PCMs) based on anorthite ceramic and cordierite ceramic for solar energy storage. Solar Energy Materials and Solar Cells 251 (2023) 112114.
[17] Argyrios Anagnostopoulos, Maria Elena Navarro, Maria Stefanidou, Panos Seferlis, Georgios Gaidajis, Yulong Ding. Effect of carbon on the performance of red mud-molten salt composites for thermal management and waste heat recovery applications. Journal of Energy Storage 44 (2021) 103363.
[18] Argyrios Anagnostopoulos, Maria Elena Navarro, Maria Stefanidou, Yulong Ding, Georgios Gaidajis. Red mud-molten salt composites for medium-high temperature thermal energy storage and waste heat recovery applications. Journal of Hazardous Materials 413 (2021) 125407.
[19] Haoran Wang, Xiaofeng Ran, Yajuan Zhong, Linyuan Lu, Jun Lin, Gang He, Liang Wang, Zhimin Dai. Ternary chloride salt-porous ceramic composite as a high-temperature phase

change material. Energy 238 (2022) 121838.
[20] Junwan Liu, Qianhao Wang, Ziye Ling, Xiaoming Fang, Zhengguo Zhang. A novel process for preparing molten salt/expanded graphite composite phase change blocks with good uniformity and small volume expansion. Solar Energy Materials and Solar Cells 169 (2017) 280-286.
[21] Qi Li, Wenzhen Wei, Yuying Li, Chuan Li, Ruihuan Ge, Yanping Du, Xinjing Zhang, Yuting Wu. Development and investigation of form-stable quaternary nitrate salt based composite phase change material with extremely low melting temperature and large temperature range for low-mid thermal energy storage. Energy Reports 8 (2022) 1528-1537.
[22] Cha-xiu Guo, Gao-lin Hu, Zhi-jun Luo. Preparation and thermal properties of graphite foam/eutectic salt composite as a phase change energy storage material. Carbon 93 (2015) 1087.
[23] Chuan Li, Qi Li, Ruihuan Ge. Comparative investigation of charging performance in shell and tube device containing molten salt based phase change materials for thermal energy storage. Case Studies in Thermal Engineering 43 (2023) 102804.
[24] Adio Miliozzi, Manila Chieruzzi, Luigi Torre. Experimental investigation of a cementitious heat storage medium incorporating a solar salt/diatomite composite phase change material. Applied Energy 250 (2019) 1023-1035.
[25] Hamoon Hemmatpour, Vahid Haddadi-Asl, Fatemeh Khanipour, Marc C.A. Stuart, Liqiang Lu, Yutao Pei, Hossein Roghani-Mamaqani, Petra Rudolf. Mussel-inspired grafting pH-responsive brushes onto halloysite nanotubes for controlled release of doxorubicin. European Polymer Journal 180 (2022) 111583.
[26] Ram Kumar Deshmukh, Lokesh Kumar, Kirtiraj K. Gaikwad. Halloysite nanotubes for food packaging application: A review. Applied Clay Science 234 (2023) 106856.
[27] Jing Ouyang, Zheng Zhou, Yi Zhang, Huaming Yang. High morphological stability and structural transition of halloysite (Hunan, China) in heat treatment. Applied Clay Science 101 (2014) 16-22.
[28] Moyun Kang, Yuqi Liu, Chenchen Liang, Wei Lin, Changxiang Wang, Chaojie Li, Feng Zhang, Jiaji Cheng. Phase change material microcapsules with DOPO/Cu modified halloysite nanotubes for thermal controlling of buildings: Thermophysical properties, flame retardant performance and thermal comfort levels. International Journal of Heat and Mass Transfer 207 (2023) 124045.
[29] Tiantian Zhang, Shi Juan, Wang Yi, Zhenqian Chen. A novel form-stable phase change material based on halloysite nanotube for thermal energy storage. Journal of Energy Storage 45 (2022) 103703.
[30] Sarinthip Thanakkasaranee, Jongchul Sel. Effect of halloysite nanotubes on shape stabilities of polyethylene glycol-based composite phase change materials. International Journal of Heat and Mass Transfer 132 (2019) 154-161.
[31] Xiaobin Gu, Lihua Peng, Peng Liu, Liang Bian, Boxuan Wei. Enhanced thermal properties and lab-scale thermal performance of polyethylene glycol/modified halloysite nanotube form-stable phase change material cement panel. Construction and Building Materials 323 (2022) 126550.
[32] Qinghua Yu, Zhu Jiang, Lin Cong, Tiejun Lu, Bilyaminu Suleiman, Guanghui Leng, Zhentao Wu, Yulong Ding, Yongliang Li. A novel low-temperature fabrication approach of composite phase material for high temperature thermal energy storage. Applied Energy 237 (2019) 367-377.

[33] Zhiwei Ge, Feng Ye, Yulong Ding. Composite materials for thermal energy storage: Enhancing performance through microstructures. ChemSumChem 7 (2014) 1318-1325.